



ELSEVIER

Available online at www.sciencedirect.com

SCIENCE @ DIRECT®

Microelectronic Engineering 78–79 (2005) 429–435

MICROELECTRONIC
ENGINEERING

www.elsevier.com/locate/mee

Artificially inscribed defects in opal photonic crystals

Fredrik Jonsson ^{a,*}, Clivia M. Sotomayor Torres ^a, Jörg Seekamp ^b,
Moritz Schniederger ^b, Anne Tiedemann ^b, Jianhui Ye ^c, Rudolf Zentel ^c

^a National Microelectronics Research Centre, University College Cork, Lee Maltings, Prospect Row, Cork, Ireland

^b Institut für Materialwissenschaften, Bergische Universität, D-42119 Wuppertal, Germany

^c Institut für Organische Chemie, Johannes Gutenberg Universität, D-55099 Mainz, Germany

Available online 13 January 2005

Abstract

Opals are three-dimensional photonic crystals, self-assembled from dielectric spherical beads into a face-centered cubic lattice. By introducing intentional defects in the crystal lattice, one modifies features such as spontaneous emission and the directionality of diffracted light. We here present a method for the artificial introduction of a lattice of such intentional defects in self-assembled poly(methyl methacrylate) (PMMA) photonic crystals by means of electron beam lithography. The inscribed defects are of the size of an individual bead, providing a broad spectral range between adjacent resonance peaks. This opens for devices with single line transmission in the photonic band gap, as well as for applications in modification and control of the diffraction properties and directionality of scattered light.

© 2005 Elsevier B.V. All rights reserved.

Keywords: Electron beam lithography; Self assembled photonic crystals; Diffraction optics

1. Introduction

In optical physics the research field of photonic crystals has during the last years gained considerable interest. The photonic crystals are, generally speaking, media possessing a periodic modulation of the refractive index, in one, two, or three dimensions, and their possibility of separating spectral

domains of light and possibility of suppressing spontaneous emission are key issues in applications for optical switching and light generation [1]. In this respect the opals are of particular interest since they provide a three-dimensional photonic structure enabling a full three-dimensional photonic band gap, which effectively can prohibit the spontaneous emission in light-matter interaction [2]. The opals are made of dielectric spheres, self-assembled into a face-centered cubic lattice [3], and due to their simplicity in fabrication they are highly scalable also up to macroscopic sizes, of the millimeter order.

* Corresponding author. Tel.: +353 21 4904391; fax: +353 21 4904058.

E-mail address: fredrik.jonsson@nmrc.ie (F. Jonsson).

In many applications of photonic crystals, it is desirable to introduce intentional defects of the crystal lattice [4]. These defects can effectively work as resonant cavities, spectrally selecting certain wavelength regions of the light as well as altering the diffraction and band gap properties of the crystal [5,6]. In particular, defects and other structural phase jumps of the crystal lattice introduce a selectivity and means of control of the spontaneous emission, being crucial for controlling the luminescence and lasing properties of active photonic crystals. For example, bi-layered luminescent opals, with two opals of different lattice parameters grown on top of each other, have proven to possess a highly anisotropic spectral response, attributed to the photonic band gap mismatch between the two opal layers [7,8].

With the exception of a few studies involving nano-robotics for the artificial assembly and structuring of opal-like crystals [9], the issue of fabrication of single-site defects in self-assembled photonic crystals has up to this point not yet been solved. One step towards the fabrication of such defects has though recently been presented [10], in which void areas were fabricated in polymeric opals using regular electron beam lithography. Due to the inherent difficulty of alignment of the writing field of the electron beam relative to the opal lattice, this work was restricted to a number of certain geometric shapes and the investigation of the relation between the control parameters in the lithography. The major conclusion of this work was that the acceleration voltage of the electron beam is the most critical parameter, with low acceleration voltages giving shallow and round shapes in the crystal, while high acceleration voltages give sharp and deep shapes [10].

2. Experimental procedure

In this paper, we present an extension of the approach of using electron beam lithography for the fabrication of defect sites in opals as voids down to the size of an individual bead. In particular, we show the scalability potential of the proposed method, illustrated by the fabrication of a rectan-

gular super-lattice of such defects inscribed in a macroscopic opal. The method of fabrication of the crystals with intentional defects as here described spans over a broad range of disciplines in physics and chemistry, involving the bead synthesis, substrate preparation, photonic crystal assembly by means of self-arrangement, defect inscription by means of electron beam lithography, and the subsequent chemical development of the samples.

The opal photonic crystals were self-assembled on doubly polished $\langle 100 \rangle$ silicon substrates, from a 4.0 mass percent dispersion of poly(methyl methacrylate) (PMMA) spheres in de-ionized water, using the vertical deposition technique [11] as illustrated in Fig. 1. The PMMA spheres were fabricated with a median diameter of $a = 498$ nm, using the modified surfactant free emulsion polymerization technique as described in [12,13]. The main advantage of using PMMA as medium, in form of spin-coated films, is that it is a commonly used and well known material for patterning with electron beam lithography. In addition, it possesses well known optical properties, making the design and subsequent theoretical evaluation process straightforward.

Prior to the opal growth, the silicon substrates were cleaned for 3 h in a 1:1 solution of sulfuric acid (95%) and hydrogen peroxide (30%). The

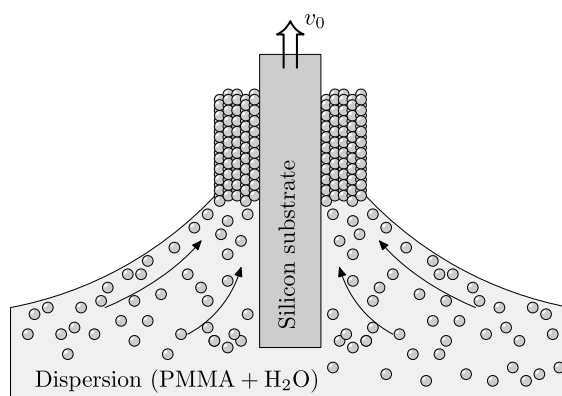


Fig. 1. The vertical deposition technique for fabrication of opal films, in which the substrate is slowly drawn with velocity v_0 from the dispersion of distilled water and PMMA beads. The forming of the face-centered lattice of the opal takes place at the meniscus formed at the dispersion–air interface at the substrate.

substrates were then hydrophilized during 3 h in a 1:1:5 agent of hydrogen peroxide (30%), ammonium hydroxide (25%), and de-ionized water, and finally blown dry with nitrogen. The opal samples were grown at room temperature and normal atmospheric pressure, at a drawing speed of $v_0 = 2.6$ mm/h, resulting in films of approximately 20 monolayers, or a thickness of $20(2/3)^{1/2}a = 8.1$ μm . The samples were then sintered at 80 °C during 1 h. Reflection spectra at normal incidence of the opal samples were measured prior to the electron beam lithography, and the first order reflection peak was found to be centered at a vacuum wavelength of 1073 nm, with a half-maximum full-width of 78 nm. The equipment used for the electron beam lithography was a Philips XL30-SFEG scanning electron microscope, equipped with a Raith Elphy Plus control unit and with a Schottky field emission gun as electron source.

The electron beam lithography used in the patterning of polymeric opals is in many respects different from the lithography used on spin-coated substrates, for example as used in fabrication of electronic components or two-dimensional silicon photonic crystals. The exposure depth is here a more critical parameter than usual, since the target process should remove exactly beads of the top layer of the opal but not more. Hence, in some sense this can be considered as an extension of the two Cartesian coordinates of the writing field to also include the writing depth as the third independent dimension to be tuned in the process.

Finally, and of most importance, contrary to the case of regular patterning of spin-coated thin polymer films on planar substrates, in which case the resist possesses a structural invariance under rotation and translation, the $\langle 111 \rangle$ surface of the opal film has a six-fold rotational symmetry and a translational periodicity of a bead diameter which the design needs to be matched to. In this alignment of the write field to the opal there are two degrees of freedom, namely the rotation of the design relative to the surface lattice of the opal, to ensure that the coordinate axes of the write field directionally coincide with those of the crystal, and the translation of the design along these axes. Both these degrees of freedom need to be tuned in order

to ensure that the exposed areas are fixed to the centers of the individual beads of the opal. In this matching, the secondary electrons of the electron beam are initially used only for the alignment, prior to the writing of the opal.

All steps in the alignment and inscription of the super-lattice of defects are performed at a constant acceleration voltage of the electron beam, and the method is as follows. First the electron beam is focused and corrected for astigmatism on a fiducial reference mark on the bare silicon substrate, outside of the opal growth area. The beam is then blanked and the substrate mount translated to center the electron beam to an area on the photonic crystal. Due to the thickness of the opal film, which causes a slight change in the actual working distance, the beam is at this point again focused in continuous scan mode, with a scan field of 15 μm and with a fast scan rate to keep the charging of the sample to a minimum. The scan area in this alignment will though be fully exposed, and is sacrificed for the sake of a sharp focus in the actual writing in a close by area. In this step, the angular orientation of the write field is also adjusted to match the opal lattice. Since the orientation of the opal lattice is quite constant over large spatial distances, this preliminary orientational alignment will still be close to optimum after a slight translation of the substrate. The beam is then again blanked and the substrate translated to an area about 30 μm from the previous point. The orientation and translation of the write field is now again checked against the opal lattice. However, this time the electron beam is operated in single scan mode, with each scan exposing the opal lattice with less than 2 $\mu\text{A s/cm}^2$. This low dose of exposure ensures that a few scans may be sampled without destroying the top layer of the opal. By finally adjusting the orientation and by locking the design lattice to match the spatial phase of the opal lattice, the alignment is finished and the exposure is started.

During the alignment it is necessary to keep the exposure to a minimum, not only because the final alignment area otherwise would be removed in the subsequent development, but also since the charge transport away from the area of exposure is low for the comparatively thick dielectric opal film.

The latter implies a considerable charging under long exposures, causing a low visibility in the alignment procedure.

The design chosen for the inscription of defects was a rectangular (mod 2) super-lattice, as illustrated in Fig. 2, with the defects appearing periodically with $2a$ and $3^{1/2}a$ in orthogonal Cartesian directions. In evaluation, this choice of super-lattice has the advantage that its surface diffraction pattern, as being the signature of the lattice of defects, possesses two-fold rotational symmetry around the normal $\langle 111 \rangle$ -axis of the face-centered cubic lattice of the opal. This fingerprint is hence easily distinguished from the six-fold rotational symmetry of the unpatterned, naturally grown crystal.

In the context of inscription of single-site defects, the acceleration voltage of the electron beam is the critical parameter, controlling the penetration depth as well as the transverse extent of the cloud of scattered electrons inside the individual beads. The optimal acceleration voltage for removal of single beads was found to be 5.5 kV, and the corresponding optimal exposure dose was $95 \mu\text{As}/\text{cm}^2$. For a super-lattice of 200×200 defect sites, covering an area of approximately $200 \times 173 \mu\text{m}^2$, the total writing time was 14 min. After the exposure, the samples were developed during 20 s in a 1:3 solution of 4 methyl-2 pentanone (methyl isobutyl ketone) and isopropanol, followed by 20 s rinse in isopropanol. After development the samples were immediately dried with nitrogen gas.

3. Results

A representative scanning electron microscope image of a typical sample fabricated by the here described method is shown in Fig. 3. From this figure, the quality of the fabricated crystal can be assessed from the fact that the second layer of the opal, of a face-centered cubic structure, is clearly visible in the sites of the defects. As also can be seen in the figure, the second layer is left virtually without impact from the electron beam lithography, proving that the set of control parameters in the electron beam lithography is close to optimum. At some sites, the stochastic fluctuations in spatial phase of the lattice has caused the beads to be only partially exposed, hence leaving hemi-spherical shells. One such shell can be seen in the upper middle of Fig. 3. More serious, the spatial phase of the crystal lattice is radically changed over cracks appearing in the opal, as shown in Fig. 4. Since these cracks appear with a period of approximately $50 \mu\text{m}$, the areas with control of a correctly matched super-lattice of defects is essentially limited to this distance. However, in many cases this issue is not as critical as it may appear, since the orientation of the opal lattice is essentially unaltered over the cracks, and the lattice displacement over the cracks often leaves an acceptable phase matching to the design lattice over larger distances.

In this work, we have chosen to use PMMA beads that give a resonance in normal reflection in the infrared region. However, the use of such beads,

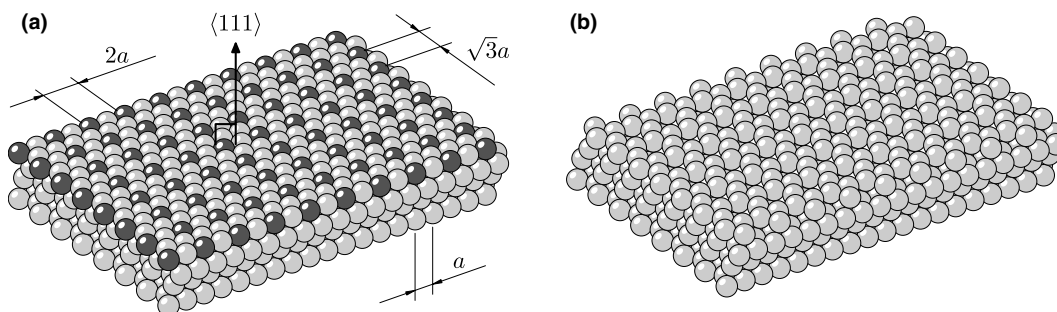


Fig. 2. (a) The exposed rectangular super-lattice of defects, schematically shown as dark spheres in the three-dimensional opal structure, and (b) the resulting inscribed defects after development, in which the exposed sites are removed. The super-lattice of defects is in terms of the opal lattice parameter a periodic with $2a$ and $3^{1/2}a$ in orthogonal Cartesian directions.

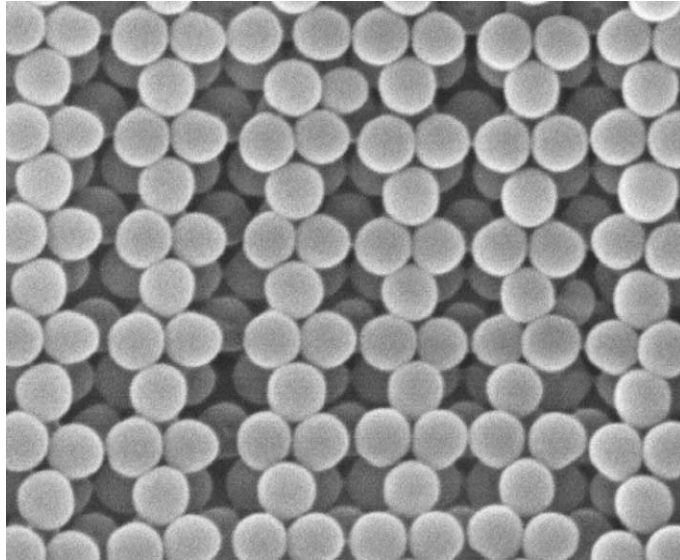


Fig. 3. Scanning electron microscope image of a gold-coated rectangular lattice of defects inscribed in the three-dimensional crystal of opal structure. The second layer of the face centered cubic lattice of beads is displayed in the sites of open defects. The median bead diameter (opal lattice parameter) is $a = 498$ nm.

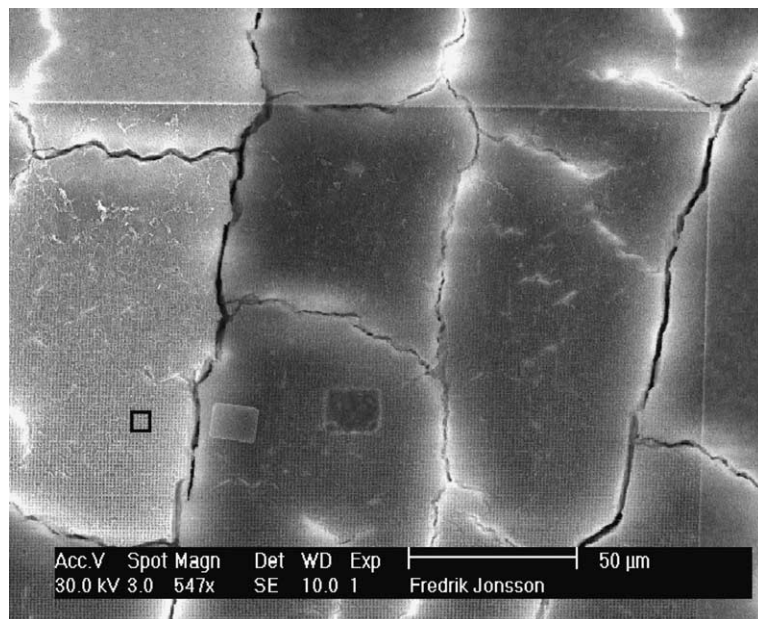


Fig. 4. Larger view of the writing area as shown in Fig. 3. In the figure, the area covered by Fig. 3 is shown with a black rectangle. To the right of this rectangle, the areas in which final focussing and astigmatism correction were performed appear as two rectangular (overexposed) domains. The angled corner in the upper right part of the image is the boundary of the inscribed super-lattice of defects, in total extending over an area of approximately $200 \times 173 \mu\text{m}^2$.

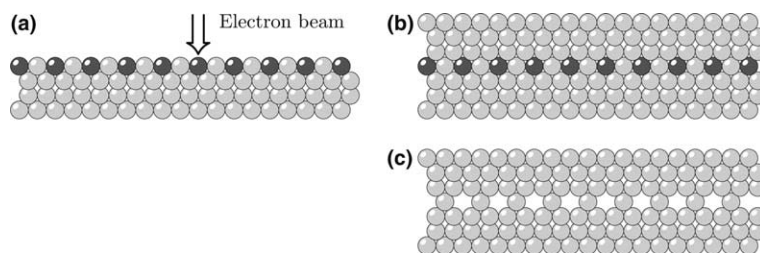


Fig. 5. The proposed three-step process to fabricate buried defects, involving (a) electron beam lithography on the opal surface, (b) deposition of a second opal layer on top of the written one, and (c) development of exposed sites, resulting in a lattice of buried defects.

which are larger than the ones as otherwise used for resonances in the visible region [14], imposes difficulties in two respects. First, it is harder to achieve a high monodispersity in the fabrication of larger beads and, second, due to the lower Brownian motion of larger beads they also have a lower tendency to stay in a homogeneous dispersion, with a much more pronounced tendency to earlier sediment towards the bottom. The latter issue is here critical, since it is necessary to keep the concentration of the beads in the dispersion constant also at the surface, and in particular in the region where the meniscus is formed in the self-assembly of the opal in the vertical deposition (Fig. 1). To solve this issue, it was found that by increasing the dispersion temperature to 60 °C the spatial homogeneity of the grown opal was improved considerably. The physical reason for this improvement is that not only the Brownian motion of the beads in the dispersion is increased, but also most probably, the temperature difference to the surrounding environment at room temperature also causes a slow laminar flow in the dispersion, keeping the homogeneity and preventing sedimentation.

4. Outlook

The main impact of the presented method of inscription of intentional defects is that it opens for the fabrication of self-assembled photonic crystals with buried defects, as illustrated in Fig. 5. In this three-stage process an additional opal film is deposited on top of the exposed opal prior to development. After the second deposition and a second sintering, the exposed sites are developed to give the desired buried defects.

5. Conclusion

In conclusion, we have presented a method for the fabrication of lattices of intentional defects in three-dimensional self-assembled PMMA photonic crystals. The presented method has proven to possess capability for inscription of defect sites down to the size of an individual bead, being approximately half a micrometer. Advantages with the presented method are that it employs standard processes for electron beam lithography, and that it is scalable to large areas. The main impact is that the process may be extended for the fabrication of buried single-site defects in self-assembled photonic crystals.

Acknowledgements

This work was supported by the EU IST-510162 Project PHAT, the Science Foundation Ireland, and the Deutsche Forschungsgemeinschaft focus programme Photonic Crystals SPP1113.

References

- [1] K. Sakoda, *Optical Properties of Photonic Crystals*, Springer-Verlag, New York, 2001, ISBN 3-540-41199-2.
- [2] E. Yablonovitch, *Phys. Rev. Lett.* 58 (1987) 2059.
- [3] C. Kittel, *Introduction to Solid State Physics*, sixth ed., Wiley, New York, 1986, ISBN 0-471-87474-4.
- [4] J.D. Joannopoulos, P.R. Villeneuve, S. Fan, *Nature* 386 (1997) 143.
- [5] M. Okano, A. Chutinan, S. Noda, *Phys. Rev. B* 66 (2002) 165211.

- [6] I. Alvarado-Rodriguez, E. Yablonovitch, *J. Appl. Phys.* 92 (2002) 6399.
- [7] V.G. Solovyev, S.G. Romanov, C.M. Sotomayor Torres, M. Müller, R. Zentel, N. Gaponik, A. Eychmüller, A.L. Rogach, *J. Appl. Phys.* 94 (2003) 1205.
- [8] N. Gaponik, A. Eychmüller, A.L. Rogach, V.G. Solovyev, C.M. Sotomayor Torres, S.G. Romanov, *J. Appl. Phys.* 95 (2004) 1029.
- [9] F. Garcia-Santamaria, H.T. Miyazaki, A. Urquia, M. Ibisate, M. Belmonte, N. Shinya, F. Mesegner, C. Lopez, *Adv. Mater.* 14 (2002) 1144.
- [10] P. Ferrand, M. Egen, R. Zentel, J. Seekamp, S.G. Romanov, C.M. Sotomayor Torres, *Appl. Phys. Lett.* 83 (2003) 5289.
- [11] Z.Z. Gu, A. Fujishima, O. Sato, *Chem. Mater.* 14 (2002) 760.
- [12] M. Müller, R. Zentel, T. Maka, S.G. Romanov, C.M. Sotomayor Torres, *Chem. Mater.* 12 (2000) 2508.
- [13] M. Egen, R. Zentel, *Chem. Mater.* 14 (2002) 2176.
- [14] S.G. Romanov, T. Maka, C.M. Sotomayor Torres, M. Müller, R. Zentel, D. Cassagne, J. Manzanares-Martinez, C. Jouanin, *Phys. Rev. E* 63 (2001) 056603.